

Asiaticoside delays senescence and attenuate generation of ROS in UV-exposure cells through regulates TGF- β 1/Smad pathway

HONGHAO JIANG, XIAOYONG ZHOU and LIUQING CHEN

Department of Dermatology, Wuhan No. 1 Hospital, Wuhan, Hubei 430030, P.R. China

Received March 13, 2022; Accepted July 8, 2022

DOI: 10.3892/etm.2022.11603

Abstract. Asiaticoside, isolated from *Centella asiatica*, shows great improvement on wound healing and anti-oxidation function *in vitro* and *in vivo*. From previous research, asiaticoside possesses the potential capability to delay skin aging and reduce wrinkles clinically, but its underlying mechanism to regulate aging have not well-investigated. The present study found that asiaticoside could improve the viability and maintains a normal morphology in ultraviolet (UV)-exposure cells. In addition, β -galactosidase release was inhibited by treatment of asiaticoside in UV damaged cells was observed. The present study confirmed that UV-induced ROS generation and SOD reduction could be attenuated by incubation of asiaticoside. By using RNA sequencing technology, differential genes between UV and asiaticoside treatment were demonstrated and enriched genes suggested that asiaticoside is able to negatively regulate cell cycle and MAPK pathways. Western blotting was employed to clarify the variation of key proteins in TGF- β 1/Smad pathway and cell cycle and the result implied that asiaticoside is capable of attenuating upregulation of TGF- β 1, Smad2 and Smad3 to reverse cell senescence. The present study investigated regulation of asiaticoside to TGF- β 1/Smad pathway in UV-induced HaCat cells, showing its potential to against photoaging.

Introduction

Photoaging is the phenomenon of skin aging or accelerated aging due to prolonged sun exposure (1). Photoaging from intense ultraviolet (UV) rays is more likely to make the skin rough, sagging, wrinkled, hyperpigmented and even precancerous, benign or malignant (2). In addition to natural aging caused by the body's natural cell metabolism, photoaging

is the second largest cause of skin aging. UV radiation can affect the formation of type I collagen, resulting in a relative increase in type III collagen (3,4), which eventually leads to a decrease in mature collagen bundles and skin laxity and wrinkles. Components of the skin's dermal matrix, such as aminoglycans and proteoglycans, are also implicated in photoaging (5). Sunlight exposure can cleave aminopolysaccharides and increase their solubility, thereby affecting their structure and function (6). UV radiation in sunlight does not directly damage the dermal matrix components. ROS are naturally generated in various biochemical reactions within organelles such as the endoplasmic reticulum, mitochondria and peroxisomes. Under normal physiological conditions, ROS are related to life activities such as cell signal transduction, cell cycle and cell proliferation. Abnormally, ROS levels in cells are elevated after being subjected to UV exposure compared with healthy cells. Due to the high activity of ROS, cells generate oxidative stress, leading to dysfunction (7). It is generally believed that UV irradiation can cause mtDNA damage, generate oxygen free radicals ROS, further lead to the oxidation of proteins in the dermal matrix and cause cellular inflammation (7,8). In turn, the matrix components are slowly dissolved. Additionally, the connection between UV exposure and senescence has been reported; that excessive UV exposure leads more expression of aging-related genes and generation of β -galactosidase in cells, indicating senescence induced by excessive UV exposure (9-11).

Centella asiatica is a perennial herb of the *Umbelliferae* family (12). A traditional Chinese medicinal plant with a long history, *Centella asiatica* is used externally to remove scars and reduce inflammation (13). The main active components of *Centella asiatica* are asiaticoside, madecassoside, asiatic acid and madecassolic acid, although their proportions in the active components has yet to be reported. Most of the active ingredients in *Centella asiatica* are triterpenoids (12). Among them, asiaticoside is the main active ingredient in *Centella asiatica* because of its rich pharmacological activity and broad clinical effects. According to scientific reports, asiaticoside demonstrates potential capability to delay skin aging and reduce wrinkles clinically (14-16). Therefore, asiaticoside has good application prospects and potential for development. Asiaticoside may be able to promote wound healing, scar removal and other skin disease treatments (17-19). However, the anti-photoaging effects of asiaticoside on skin and the potential mechanisms of action remain to be elucidated.

Correspondence to: Professor Liuqing Chen or Professor Xiaoyong Zhou, Department of Dermatology, Wuhan No. 1 Hospital, 215 Zhongshan Avenue, Wuhan, Hubei 430030, P.R. China
E-mail: chlq35@126.com
E-mail: zhouxuefeng1970@126.com

Key words: ultraviolet exposure, asiaticoside, HaCat cells, cell stress, reactive oxygen species, TGF- β 1/Smad pathway, p53

In the present study, the therapeutic effects of asiaticoside on skin photoaging and possible molecular mechanisms were investigated by analyzing the modulation of appearance, cell structure, oxidative stress, pigmentation index and related proteins in a cellular photoaging model.

Materials and methods

Materials. HaCat cells were purchased from Procell Life Science & Technology Co., Ltd. (cat. no. CL-0090) and verified by using short tandem repeat (STR) profiling. Asiaticoside was obtained from MilliporeSigma. Primers used in this study were synthesized by Sangon Biotech Co., Ltd. All the antibodies were purchased from Cell Signaling Technology, Inc.: TGF- β (56E4) Rabbit mAb cat. no. 3709 (1:1,000); Smad2 (D43B4) XP Rabbit mAb cat. no. 5339 (1:1,000); Smad3 (C67H9) Rabbit mAb cat. no. 9523 (1:1,000), p53 (DO-7) Mouse mAb cat. no. 48818 (1:1,000), p21 Waf1/Cip1 (12D1) Rabbit mAb cat. no. 2947 (1:1,000), MMP-9 (D6O3H) XP Rabbit mAb cat. no. 13667 and GAPDH (D16H11) XP[®] Rabbit mAb cat. no. 5174 (1:2,000).

Cell culture. A human keratinocyte cell line (HaCat cell) was used in all the experiments. HaCat cells were cultured by using Dulbecco's modified eagle medium (DMEM) with 10% (v/v) fetal bovine serum containing 1% (v/v) penicillin and streptomycin (Thermo Fisher Scientific, Inc.).

Cell counting kit-8 assay (CCK-8). The viability of HaCat cells after UV exposure and incubation with asiaticoside in low, medium and high doses was determined by using CCK assay (Beijing Solarbio Science & Technology Co., Ltd.) following the manufacturer's protocol (20,21). In brief, 2×10^4 cells were suspended in 200 μ l DMEM medium and then seeded in a 96-well transparent-bottom plate and cultured in an incubator at 37°C for 24 h. The culture medium in the wells was replaced by fresh medium before administration of UV exposure (UV-B, 100 mJ/cm², λ_{\max} =312 nm) and incubation with asiaticoside in different doses at 37°C (low concentration: 1 mg/l, medium concentration: 10 mg/l and high concentration 30 mg/l). At 24, 48 and 72 h after UV exposure, 20 μ l CCK solution was added to the wells and cell viability of various groups were observed by a microplate reader at 450 nm after treatment of CCK solution with cells for 1 h. The absorbance of untreated cells (wildtype group, WT) served as a negative control in this experiment.

Morphological investigation. After UV treatment, the genome of some HaCat cells was disrupted leading to the activation of stress systems, which in turn caused changes in cell morphology. The present study investigated the protective effect of pretreatment of asiaticoside on cells subjected to UV stimulation by observing cell morphology. Control HaCat cells (1×10^5) were seeded to 6-wells plate and cultured at 37°C overnight. The culture medium was replaced and cells were subjected to a UV exposure for 30 min, while administration of asiaticoside with various doses was implemented 2 h before UV treatment. At 24 h following UV expose, morphological data of different groups were acquired by using an optical imaging system (CX41; Olympus Corporation).

Detection of activity of β -galactosidase. To calculate the activity of senescence-related β -galactosidase induced by UV exposure and its activity in HaCat cells following asiaticoside administration in various doses, senescence β -galactosidase staining kit (Beyotime Institute of Biotechnology) was used to count the number of β -galactosidase positive cells. HaCat cells (1×10^5) were seeded into a 6-well plate and cultured at 37°C overnight. Following UV exposure and incubation of asiaticoside in various doses, medium was removed and cells were rinsed by fresh PBS buffer and then fixed using the fixative from the kit for 15 min at room temperature. Cells were cleaned by PBS for three times following fixation and underwent incubation with staining buffer for overnight at 37°C atmosphere. Parafilm was used to cover the plate to prevent evaporation of the buffer. Images were captured using an optical microscope at x200 magnification (CX41; Olympus Corporation) and data was analyzed by using ImageJ software (v1.8.0, National Institutes of Health).

Investigation on reactive oxygen species (ROS). ROS can be induced when cells encounter stress such as exposure to heat and UV. To clarify the protective capability of asiaticoside to UV-induced skin damage, flow cytometry (Beckman Coulter, Inc.) was used to identify the ratio of ROS positive cells in the groups treated with asiaticoside in various concentrations. Cells were stained by 2',7'-dichlorofluorescein diacetate (DCFH-DA) probe for facilitating flow cytometric cell sorting assay. Briefly, 1×10^5 HaCat cells were seeded to 6-wells plate and cultured at 37°C overnight and then 1 ml DCFH-DA dye which was diluted to 10 μ M/l as a working concentration by using culture medium without FBS was added to cells following administration of UV and incubation of asiaticoside for 20 min at 37°C. Following staining, cells were rinsed by pre-warmed (37°C) culture medium for three times to remove free DCFH-DA dye. ROS-positive cells were identified and determined by observing the intensity of fluorescence in the FITC channel and HaCat cells without any treatments were used as a negative control. FlowJo software (v10.5.3, FlowJo LLC) and ImageJ (v1.8.0, National Institutes of Health) were employed to analyze and visualize data.

Determination of superoxide dismutase (SOD). SOD is a metalloenzyme widely found in living organisms and is an important scavenger of oxygen radicals, catalyzing the dismutation of superoxide anions to produce H₂O₂ and O₂. SOD is not only a superoxide anion scavenger but also a major H₂O₂ producing enzyme, which has an important role in the biological antioxidant system. To investigate the protection capacities of asiaticoside in various doses to UV-exposed HaCat cells, SOD activity assay kit (Beijing Solarbio Science & Technology Co., Ltd.) was used following manufacturer's protocol. In short, 1×10^5 HaCat cells were seeded into 6-wells plate and cultured at 37°C overnight. Cells were subjected to UV exposure for 30 min, while cells in asiaticoside treated groups were preincubated with asiaticoside in different doses for 2 h before UV exposure. Following administration of asiaticoside and UV, cells were rinsed by pre-chilled (4°C) PBS buffer and disassociated by EDTA-trypsin buffer. Disassociated cells were centrifuged at 800 x g, and the supernatant was removed before sediments were resuspended by 100 μ l of lysis buffer from

the kit. A sonicator was used to split cells at 4°C (40% power, 10 sec stopping time after 10 sec of sonication for 3 times) to release intracellular SOD. Harvested lysates were subjected to a centrifugation at $\sim 7,100 \times g$, 4°C for 10 min and supernatants mixed with detection buffers. Following water bath at 37°C for 30 min, mixtures were transferred to 96-wells plate for data acquisition by using a microplate reader under 562 nm.

TdT-mediated dUTP Nick-End Labeling (TUNEL) staining. TUNEL staining was performed by using One-step TUNEL staining kit (Beyotime Institute of Biotechnology) followed manufacturer's instructions to observe the protective ability of asiaticoside to UV-induced apoptosis (22). HaCat cells (1×10^4) were seeded to confocal dishes and cultured in an incubator for 37°C overnight. HaCat cells were fixed by 4% paraformaldehyde at room temperature for 1 h following UV radiation and administration of asiaticoside in different concentrations. Next, 50 μ l of prepared staining buffer was added to confocal dish for 1 h at room temperature to label cells in early apoptosis. Then, DAPI was used to stain the nucleus following a proper washing procedure. Finally, TUNEL staining result of HaCat cells was observed and images acquired by using a confocal microscope (Carl Zeiss AG).

RNA sequencing (RNAseq) analysis. RNAseq was employed to identify and enrich the mRNAs with great expression in the WT group, UV exposure group and asiaticoside treatment following UV exposure. The experiment and data analysis were carried out at Novogene Biotech Co., Ltd. In brief, RNAs of all the samples were extracted and purified to build libraries for following sequencing. After the library was qualified, the different libraries were pooled according to the effective concentration and the target amount of data from the machine, then sequenced by the Illumina NovaSeq 6000 (Illumina, Inc.).

Index of the reference genome was built and paired-end clean reads were aligned to the reference genome by using Hisat2 (v2.0.5, <http://daehwankimlab.github.io/hisat2/main/>). Gene Ontology (GO) enrichment analysis of differentially expressed genes was implemented by the clusterProfiler R pack (<http://www.R-project.org/>). In addition, correlation of samples in different group was analyzed by using R pack (<https://cran.r-project.org/web/packages/correlation/>). The analytic tool for Gene Set Enrichment Analysis (GSEA) was from the Broad Institute (<http://www.broadinstitute.org/gsea/index.jsp>).

Reverse transcription-quantitative (RT-q) PCR. RNA was extracted from the cells following UV exposure and appropriate treatment of asiaticoside and the expression of indicated genes was detected by RT-qPCR following reverse transcription (23). In brief, total RNA was extracted from 1×10^5 HaCat cells by TRIzol[®] reagent (Thermo Fisher Scientific, Inc.) and converted to cDNA by PrimeScript RT reagent kit (Takara Bio, Inc.) according to the manufacturer's instructions. qPCR was carried out in QuantStudio 6 Flex RT-PCR System (Thermo Fisher Scientific, Inc.). The reaction conditions were as follows: 95°C for 10 min; 40 cycles of 95°C for 15 sec, 60°C for 30 sec; followed by 72°C for 5 min. The quantitation values for each target genes were expressed as $2^{-\Delta\Delta Cq}$ (24). PCR primers used to amplify the target genes were as follows: Myosin regulatory

light chain interacting protein (MYLIP) Forward: AAACAA CCAGAGCCCTTCACAC, Reverse: CTCCTCCTCGCAGCA CACC; MYC proto-oncogene (MYC) Forward: CTCCAC ACATCAGCACA ACTACG. Reverse: GTTCGCCTCTTG ACATTCTCCTC; centromere protein F (CENPF) Forward: GGAGTTACAGCAAGCCAAGAATATG, Reverse: TCT GACTCGCTGGAACGC; serum/glucocorticoid regulated kinase 1 (SGK1) Forward: GAACACAACAGCACAACA TCCAC, Reverse: AGGCACCACCAGTCCACAG; phytochrome interacting factor (PIF) Forward: GGCAGGTGT TCAGATGAGGTG, Reverse: TGAAGCCGCCTCTCGTTG G; DNA topoisomerase II alpha (TOP2A) Forward: GGG CACCAGCACATCAAAGG, Reverse: GCAGCATCATCT TCAGGACCAG; TGF- β 1 Forward: GGCCAGATCCTGTCC AAGC, Reverse: GTGGGTTTCCACCATTAGCAC; Smad2 Forward: CGTCCATCTTGCCATTACAG; Reverse: CTC AAG CTCATCTAATCGTCCTG; Smad3 Forward: TGGACGCAG GTTCTCCAAAC; Reverse: CCGGCTCGCAGTAGGTAAC; P53 Forward: CAGCACATGACGGAGGTTGT, Reverse: TCA TCCAAATACTCCACACGC. GAPDH was used as house-keeping gene, Forward: GGAGCGAGATCCCTCCAAAAT, Reverse: GGCTGTTGTCATACTTCTCATGG. qPCR data was collected from three independent experiments.

Western blotting. HaCat cells were harvested after 5 days, exposed to UV for 30 min in every 12 h and continually treated by asiaticoside with various concentration. Collected cells were lysed by RIPA lysis buffer containing protease and phosphatase inhibitors on the ice bath. After 30 min, lysates were transferred to EP tubes for a centrifugation at $\sim 15,500 \times g$ at 4°C for 10 min and the supernatant was collected for immunoblotting assay. A BCA kit was used to calculate concentration for samples to achieve normalization of sample concentrations. The same amount (30 μ g) of protein was subjected to SDS-PAGE with a 10% SDS-PAGE gel, and then transferred to polyvinylidene fluoride (PVDF) membrane by using a semi-dry transfer system (Bio-Rad Laboratories, Inc.). PVDF membranes were blocked with 5% BSA-Tris Buffered Saline with 0.05% Tween-20 (TBST) buffer at room temperature for 1 h. Primary antibodies were used to incubate the membrane overnight at 4°C and HRP coupling secondary antibody was used to incubate the membrane for 2 h at room temperature following an appropriate washing procedure, three times using TBST. The visualization of corresponding proteins was achieved by using a ECL chemiluminescence detection system and intensities of fluorescence were analyzed by ImageJ (v1.8.0, National Institutes of Health).

Statistical analysis. Data were collected from three independent samples unless mentioned otherwise and was expressed as means \pm standard deviation. Differences were identified using Dunnett's multiple comparison test following one-way analysis of variance (ANOVA) and performed using GraphPad Prism 7 (GraphPad Software, Inc.). $P < 0.05$ was considered to indicate a statistically significant difference.

Results

Protective ability of asiaticoside to damage by UV. UV exposure can break chemical bonds in the DNA, which may

cause misalignment, inversion, deletion or duplication of bases in the DNA as it is reassembled, thus altering the genetic information and eventually leading to cell death. To clarify the protective ability of asiaticoside in UV-damaged cells, CCK-8 assay was used to check the cell viability in every 24 h for 3 days.

Viability of cells in the UV exposure group was impaired which compared with WT group at all of three timepoints. Treatment of asiaticoside with low-, medium- and high concentrations achieved improvement of viability at 24, 48 and 72 h. High dose of asiaticoside following UV exposure shown the best therapeutic result among three kinds of treatment, while low concentration of asiaticoside had limited function on improvement of viability (Fig. 1). This data indicated that asiaticoside is able to protect cell viability from UV exposure and its ability to protect was concentration dependent.

Effect of treatment of asiaticoside on morphology of UV-damaged HaCat cells. It is well-known that excessive radiation of UV can induce cell apoptosis in cells. During apoptosis, the cell membrane is unable to maintain normal physiological functions and cytochrome C in mitochondria is released into the cytoplasm, activating the classical downstream cysteinyl aspartate specific proteinase (Caspase)-3 cell death pathway (25). The morphology of cells will be affected significantly during apoptotic process. Thus, optical microscopy was employed to identify the variations of WT group and asiaticoside treated groups to UV exposure.

Similar to the result of CCK-8 assay, morphological results illustrated that a number of cells died and that the area of confluence was much smaller compared with wildtype group following UV radiation. However, asiaticoside was able to ameliorate these effects and maintain more cell colonies even at a low concentration by preincubation for 2 h before UV exposure. With increasing concentrations of asiaticoside, the majority of cells survived radiation and formed more colonies (Fig. 2A). Although damaged cells treated with a high dose of asiaticoside did not regain as full confluence as the WT group, their condition greatly improved compared with UV treated group.

Asiaticoside inhibits activity of β -galactosidase following UV exposure. The release of β -galactosidase is related to cell senescence has been widely reported (9,10). As a main risk factor for photoaging of skin, UV can initiate the release of β -galactosidase in cells, resulting in activation of p16 protein and its correspondingly signaling pathway, leading to cell senescence. Thus, detecting activity of β -galactosidase in cells could testify the protective capability of asiaticoside to UV-induced β -galactosidase release.

By counting the number of positive cells under the microscope, the results clearly proved that the UV exposure promoted the production of β -galactosidase in cells and the ratio of positive cells increased from 2.2 to 34.8% in the WT group (Fig. 2B and C). Meanwhile, incubation with asiaticoside could effectively attenuate the activity of β -galactosidase and the positive ratios of asiaticoside treated groups ranges from 16.9% in the low concentration group, 9.3% in the medium concentration group and 5.9% in the high concentration group. Treatment with asiaticoside at various concentrations in

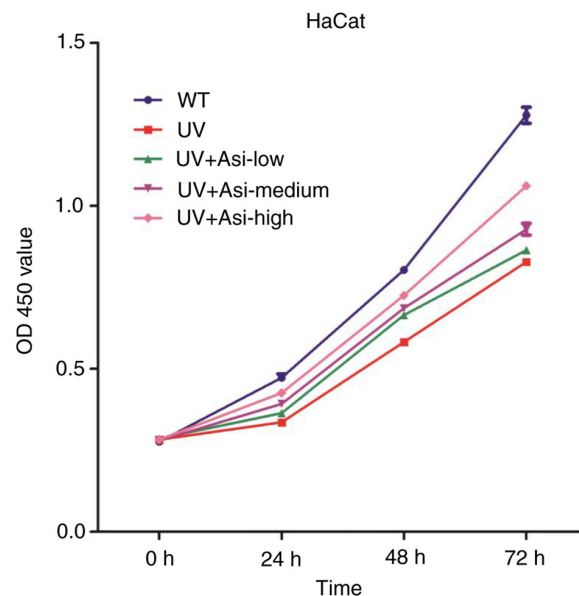


Figure 1. Viability of HaCat cells treated with UV and treatment of asiaticoside in various concentration at 24, 48 and 72 h, respectively. OD, optical density; UV, ultraviolet; WT, wildtype; Asi, asiaticoside.

control cells did not cause a significant increase of activity of β -galactosidase, implying the advantage of asiaticoside in its biosafety to healthy tissues and cells.

Asiaticoside attenuates UV-induced ROS release. UV exposure generates ROS, which are involved in body signal transduction and cellular defense mechanisms. Excessive ROS production leads to the activation of inflammation-related pathways and the release of inflammatory cytokines (26). The stimulation of cells by chronic inflammation increases the incidence of cancer (27). As a well-established carcinogenic factor, UV is a strong health threat to the public. In the present study, flow cytometric cell sorting was employed to investigate effect of asiaticoside incubation on ROS generation to UV-exposure cells.

Comparing fluorescence intensity of ROS-positive cells in UV treated group with WT group, intracellular ROS was significantly increased following UV exposure, with the ratio of ROS-positive cells from 16.8-92.8% (Fig. 2D and E). With the treatment of asiaticoside, fluorescence intensity of generated ROS was attenuated in the three groups, achieving 66.7% positive cells in low concentration group, 41.6% positive cells in medium concentration group and 26.5% positive cells in high concentration group. This result confirmed that asiaticoside was a strong inhibitor to generation of UV-induced ROS.

Ability of asiaticoside to recover activity of SOD. SOD is a natural scavenger of superoxide radicals in the body, where it can convert harmful superoxide radicals into hydrogen peroxide, which is eventually harmlessly turned into water through the action of catalase and peroxidase. Due to its ability of eliminating superoxide radicals, it could resist cell senescence induced by UV exposure. SOD activities were investigated by using a SOD activity assay kit to calculate effect of asiaticoside incubation on activity of SOD to cells damaged by UV radiation.

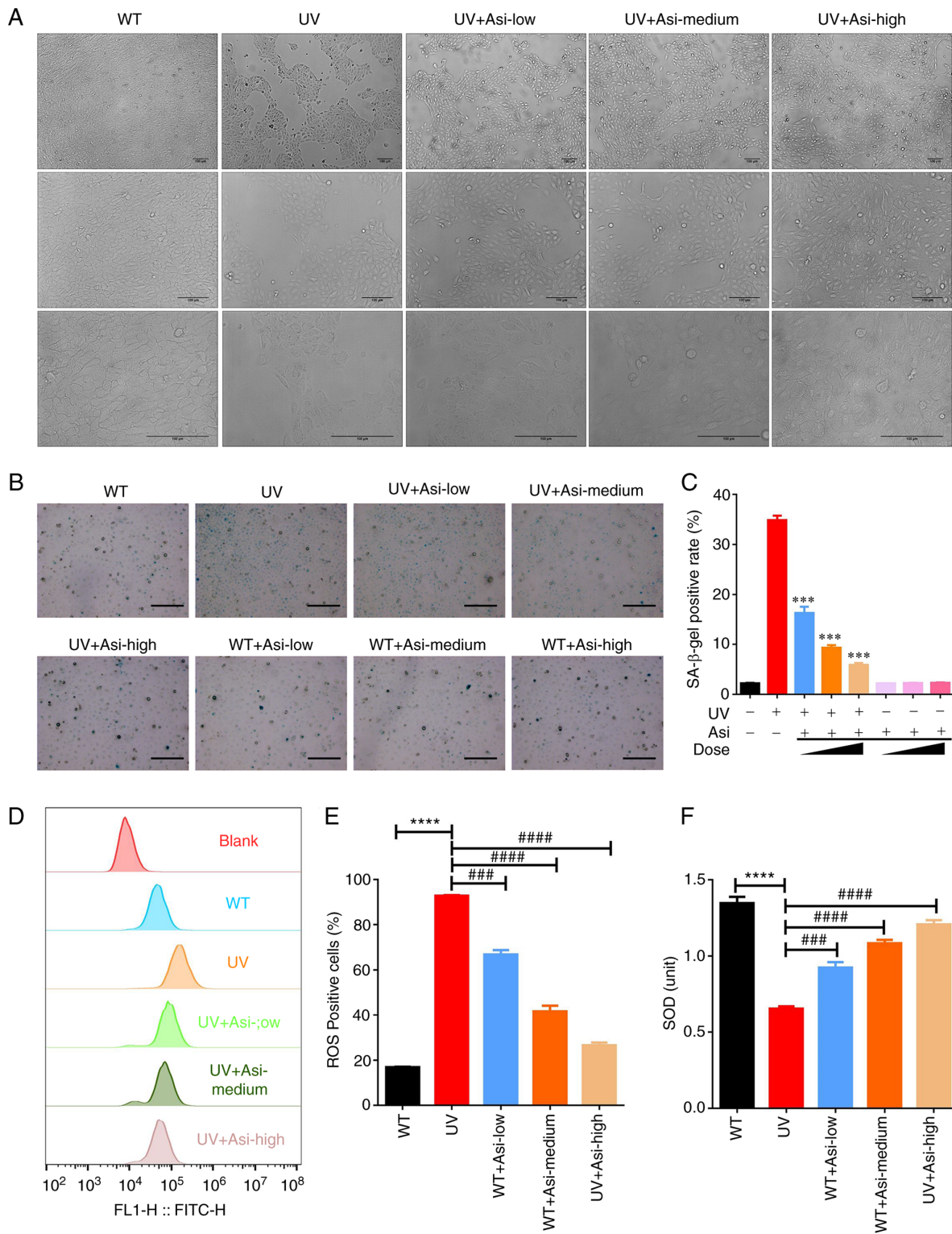


Figure 2. Asiaticoside effectively protects HaCat cells from cellular senescence induced by UV exposure. (A) Morphological results of HaCat cells after subjecting a treatment of UV and incubation of asiaticoside with various concentration for 24 h (scale bar=100 μm; magnification x100, x200 and x400 from top to bottom). (B) Detection of β-galactosidase activity in HaCat cells after UV exposure and incubation of asiaticoside with various concentration (scale bar=200 μm). (C) Corresponding analytic result of optical data to activity of β-galactosidase. (D) Flow cytometry analysis of fluorescence intensity of HaCat cells after treatment with UV and asiaticoside in various concentrations. (E) Corresponding analytic result of fluorescence intensity to ROS positive cells. (F) Analysis of SOD activity of HaCat cells after treatment with UV and asiaticoside in various concentrations. *significance of comparison between UV with WT group; #significance of comparison between treatment of asiaticoside in various doses with UV group. ***P<0.001, ****P<0.0001, ###P<0.001 and ####P<0.0001. UV, ultraviolet; WT, wildtype; Asi, asiaticoside; ROS, reactive oxygen species; SOD, superoxide dismutase.

As the results showed, activity of SOD was impaired by UV radiation following UV exposure compared with WT group

(Fig. 2F). Dramatically, incubation of asiaticoside with various concentrations achieved successfully rescue of reduction of

SOD activity in cells. Along with the increasing concentration of asiaticoside, SOD activity was improved compared with UV damaged cells and treatment of high dose of asiaticoside gained the best therapeutic result among groups treated by three doses following UV radiation.

Asiaticoside attenuates cellular apoptosis induced by UV radiation. Due to UV damage to genomic structure, damaged cells initiate apoptosis-related signaling while the broken genome can be recognized by specific probes and show fluorescent signals. In the UV group, the nucleus region exhibited a strong signal, indicating that the cells were severely damaged; however, the irradiated cells treated with asiaticoside showed a clear difference from the UV group, with the fluorescence signal being attenuated, demonstrating the protective effect of asiaticoside on UV-induced injury (Fig. 3). Notably, the number of cells undergoing apoptosis decreased with increasing asiaticoside concentrations.

Validation of correlation of samples and visualization of enriched mRNAs. The clustering results of the correlation showed that the samples in each group were significantly different from the other groups, indicating the confidence of the sequencing results (Fig. 4A). In RNA-Seq analysis, standardization of the number of read counts of genes or transcripts using Fragments Per Kilobase Million (FPKM) is an important step for sample analysis to eliminate inter-sample variation. FPKM results showed the difference in expression of partial genes occurring following UV exposure and treatment with asiaticoside compared with the WT group (Fig. 4B). Following visualization of enriched mRNAs, genes with significant variation were demonstrated. There were 2,805 downregulated and 2,828 upregulated genes in the WT group, while there were 78 downregulated and 358 upregulated genes with treatment of asiaticoside following UV radiation compared with UV group (Fig. 5A and B). By categorizing these differential genes, the number of differential genes between three groups were shown in the form of a Venn diagram and top ranked genes based on abundance were expressed in the form of heatmap (Fig. 5C and D).

GO enrichment analysis. By using GO analysis, the up- or downregulated vital activities caused by differential genes were clustered according to frequency. Following UV radiation, DNA replication and integrity checkpoints were suppressed, but protein targeting and localization to endoplasmic reticulum (ER) were upregulated in HaCat cells, indicating cells were unable to maintain normal genomic integrity and initiate a stress response through ER (Fig. 6A and B). With the treatment of asiaticoside, cell fission was inhibited and upregulation of negative regulation of MAPK cascade was observed (Fig. 6C and D). This result implied that asiaticoside could regulate cell cycle and control MAPK pathway in a negative way.

mRNA expressions of UV exposure and treatment of asiaticoside in HaCat cells. Following intense external stimulation, gene transcription is regulated in order to maintain normal cellular homeostasis and in response to transduction of signaling pathways (1,7). For quantifying transcriptional level of photoaging-related genes, RT-qPCR was used to determine

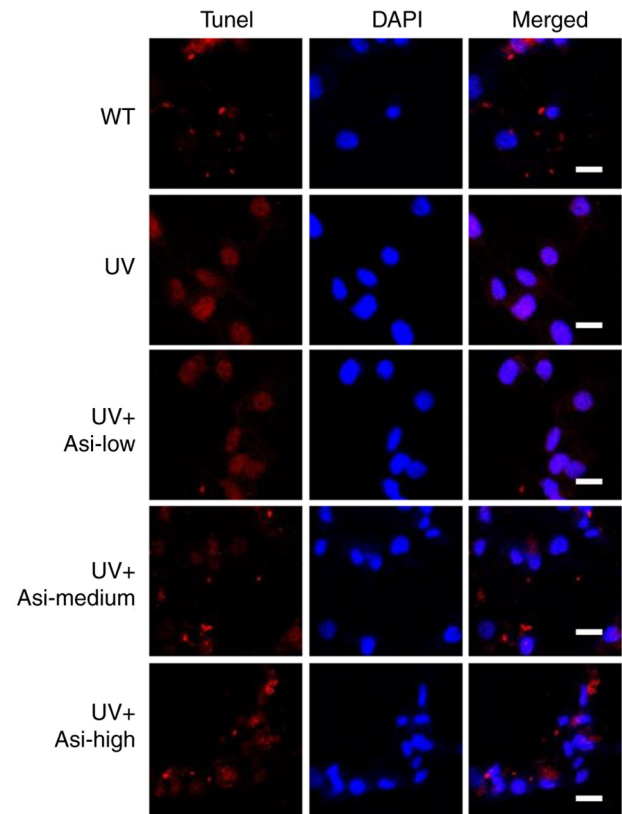


Figure 3. TUNEL staining result of HaCat cell treated with UV and administration of asiaticoside in various concentrations (scale bar=20 μ m). UV, ultraviolet; WT, wildtype; Asi, asiaticoside.

gene variation in HaCat cells following UV exposure and treatment with asiaticoside.

Following UV exposure for 30 min, cells exhibited significantly suppression of gene transcription to MYLIP, MYC and SGK1, while inhibition of three genes were induced by UV could be eased by incubation with asiaticoside (Fig. 7A, B and D). By contrast, increased transcriptional levels of CENPF, PIF and TOP2A were downregulated by treatment of asiaticoside, indicating an effective capability of asiaticoside to anti-photoaging in HaCat cells (Fig. 7C, E and F). Since functions of MYC and SGK1 are related to the cell growth, inflammation and apoptosis, asiaticoside and CENPF, PIF and TOP2A are related to genomic function, showing that asiaticoside was capable of regulating multiple cell activities and preventing damage to the genome from UV exposure. Furthermore, transcriptional levels of TGF- β 1, Smad2, Smad3 and P53 have been determined to instigate regulatory patterns of asiaticoside in cell growth factor pathway (28,29) (Fig. 7G-J). As the data suggested, increased expression of afore mentioned genes was inhibited by administration of asiaticoside at a high concentration following UV exposure, indicating the potential of asiaticoside to modulate signaling transduction of cell growth factor pathway.

Regulation of Asiaticoside on cell signaling pathways. As the RNAseq results suggested, asiaticoside inhibited TGF- β 1 family members following incubation with HaCat cells. However, the detailed signaling transduction of TGF- β 1/Smad pathway remains to be elucidated. Therefore, western blotting

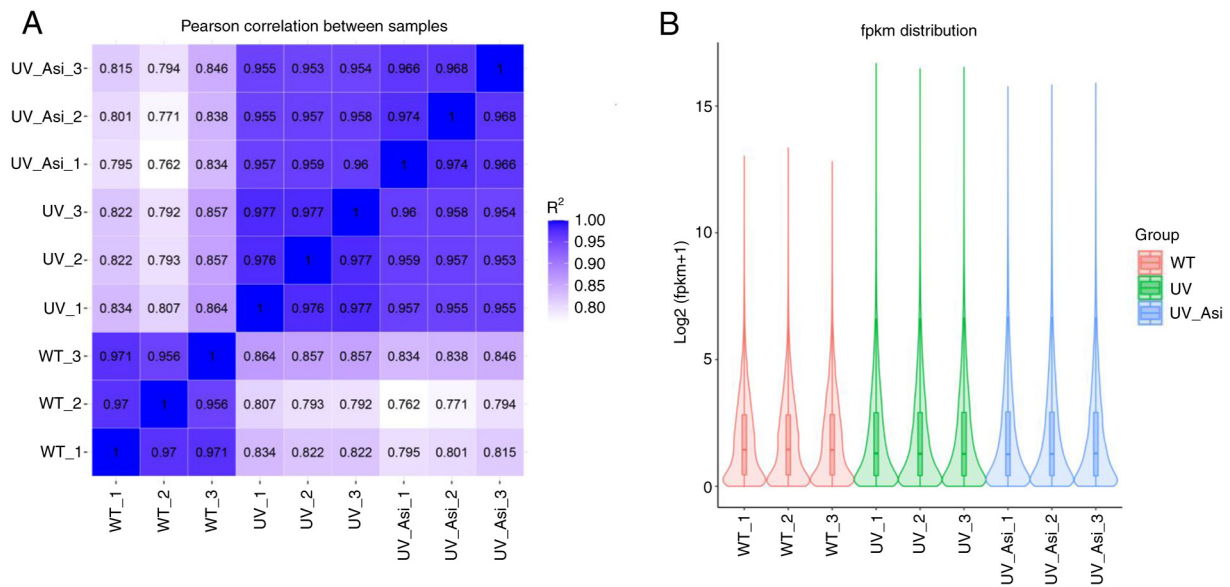


Figure 4. Clustered analysis of correlation to analyzed samples. (A) Correlation factors of all the samples. (B) Expected number of fragments per kilobase of transcript sequence per millions base pairs sequenced analysis. UV, ultraviolet; WT, wildtype; Asi, asiaticoside.

was implemented to clarify the regulation of asiaticoside to TGF- β 1/Smad pathway to understand its potential mechanism.

Cells underwent a stress response following UV radiation to generate large amounts of TGF- β 1, which enters the cell via the TGF receptor (TGFR) and phosphorylated downstream proteins Smad2/3 into the nucleus to regulate gene transcription. However, asiaticoside was able to attenuate ROS generated in response to oxidative stress and upregulated SOD activity, resulting in a decrease in intracellular TGF- β 1 expression (Fig. 8). The intensity of regulation was proportional to the concentration of asiaticoside treatment and high concentrations of asiaticoside effectively prevented ROS production, leaving TGF- β 1 expression at normal levels, which in turn affected the amount of downstream Smad2/3 proteins. Meanwhile, the expression of inflammatory protein MM9 was inhibited by asiaticoside, confirming the existence of a reduced amount of ROS in asiaticoside-treated cells. At same time, upregulated expression of cell cycle related proteins p53 and p21, which respond to DNA damage induced by UV, was significantly suppressed by incubation with asiaticoside. Due to p53 and p21 being able to stop cell cycle resulting in cell senescence and such signaling transduction could be inhibited by asiaticoside, the result of western blotting proved that asiaticoside was capable to attenuate upregulation of TGF- β 1, Smad2 and Smad3 and to reverse cell senescence.

Discussion

Aging, also known as senescence, is an inevitable stage in the process of biological life activities. It usually refers to the gradual process of functional and qualitative decline of the organism over time as the organism matures under normal conditions (30). Therefore, aging is not a disease, but a physiological phenomenon. Skin aging includes natural aging and photoaging. Photoaging is the damage to the skin caused by prolonged exposure to sunlight, characterized by rough skin, thickening, sagging, deep and coarse wrinkles and

localized hyperpigmentation or telangiectasia. Among UV, UVA and UVB are mainly involved in the pathogenic process of photoaging (31). UVB irradiation can cause skin erythema and delayed pigmentation, destroy the skin's moisturizing ability and make the skin rough and wrinkled. Long-term UVB irradiation can thicken the skin keratin and even cause melanoma (32). UVA is the main spectrum of skin tanning, its photochemical and photobiological effects are not as obvious as UVB, but the dose of UVA in sunlight is many times higher than UVB and the penetration ability is strong, penetrating deep into the skin, so UVA also has an important impact in causing skin photoaging (33,34).

UVA and UVB can both induce large amounts of ROS in the skin, causing oxidative damage to cellular structures such as DNA, proteins or lipids and enhancing oxidative stress on the skin, which in turn causes deep-seated skin damage (35). Different wavelengths of UV can induce the skin to produce different types of ROS (30). Among them, UVB mainly stimulates the production of O_2^- through the activation of NADPH oxidase and the respiratory chain reaction (36), while UVA generates H_2O_2 through the photosensitization reaction with internal chromophores such as riboflavin and porphyrin (37). Therefore, scavenging intracellular ROS can alleviate skin damage caused by UV and is also a potential target for preventing photoaging.

Centella asiatica is a traditional Chinese medicinal plant and its medical value has been affirmed. *Centella asiatica* is used as a whole herb, which is bitter in taste and acid (15). The main active components in *Centella asiatica* are asiaticoside, madecassoside and asiatic acids, its multiple functions on regulating cell activities is for attenuating damage from UV exposure (12). Studies have shown that extract of *Centella asiatica* can effectively inhibit ROS induced by TGF- β 1 in HPMC through Nrf2 activation (38,39). Therefore, the present study investigated the therapeutic effect of asiaticoside on UV-induced photoaging at the cellular level. It was found that downregulation of ROS content by asiaticoside also

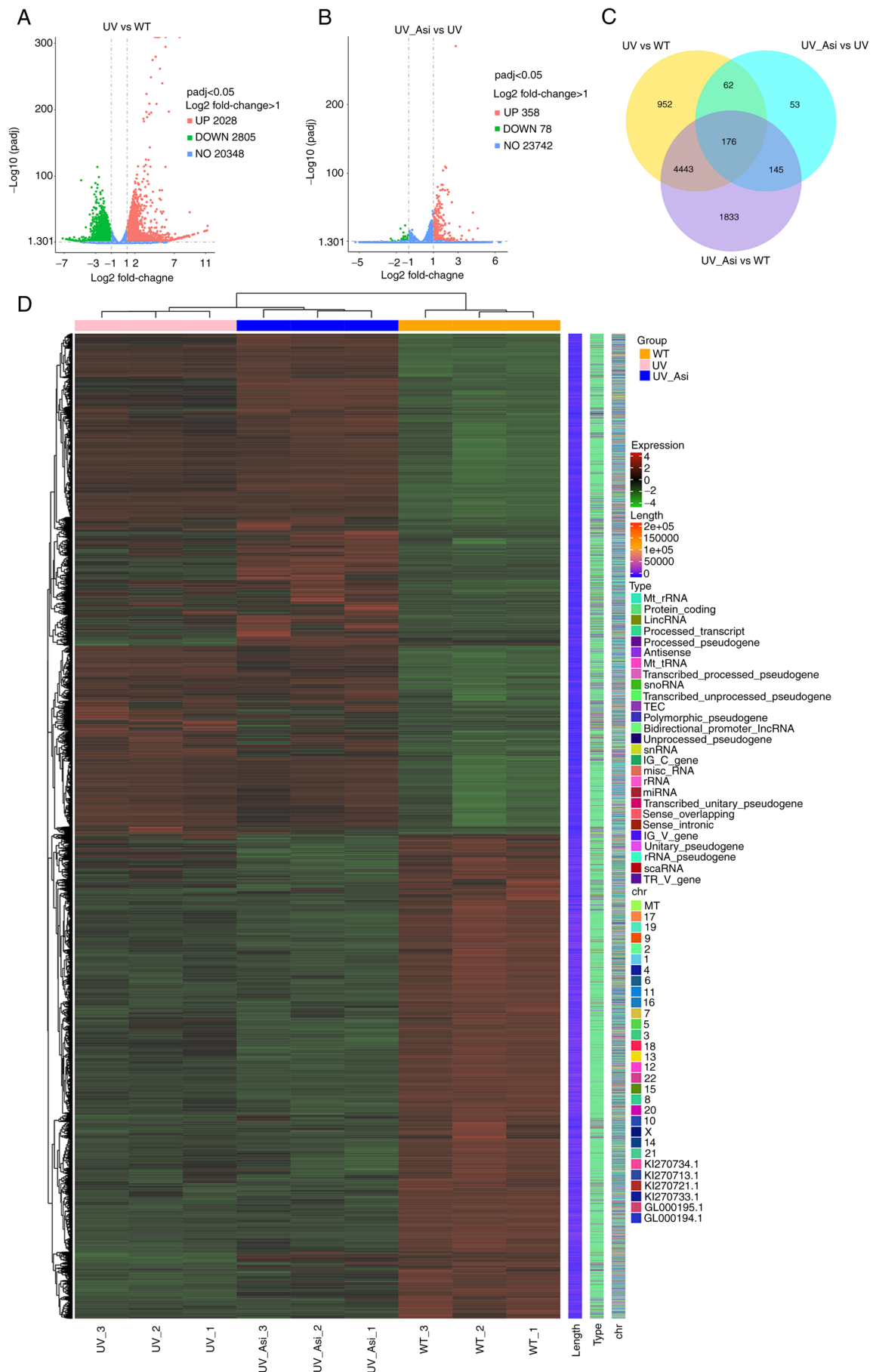


Figure 5. Visualization of enriched genes which have significant difference upon treatments. (A) Clustered genes in UV group compared with WT group. (B) Clustered genes in asiaticoside treated group compared with UV group. (C) Venn diagram of number of differential genes. (D) Heatmap of enriched genes among three groups. UV, ultraviolet; WT, wildtype; Asi, asiaticoside.

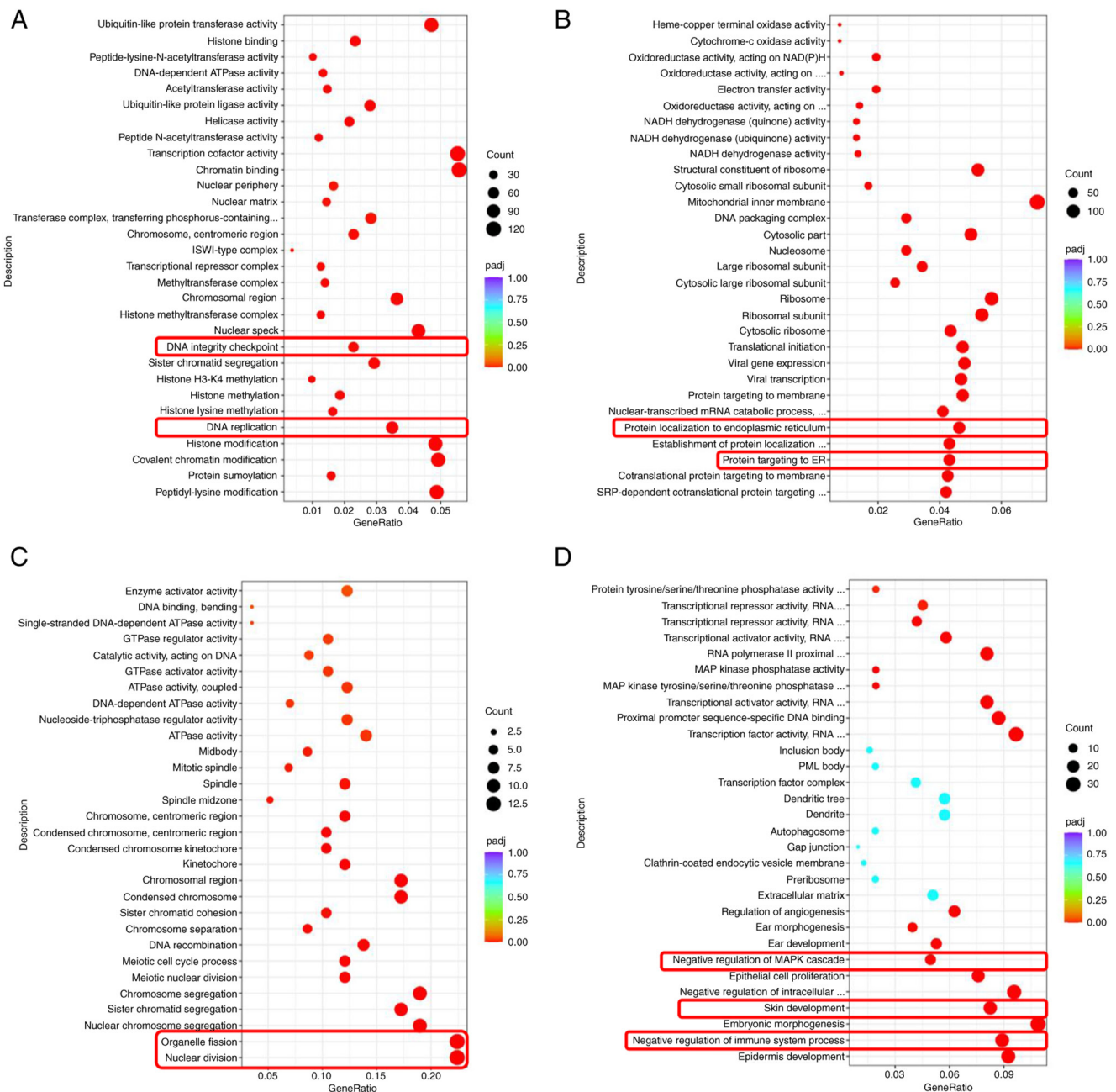


Figure 6. Analysis of enriched physiological reactions derived from Gene Ontology database. (A) Downregulated biological events in UV group vs. WT group. (B) Upregulated biological events in UV group vs. WT group. (C) Downregulated biological events in asiaticoside treated group vs. UV group (Asi + UV vs. UV). (D) Upregulated biological events in asiaticoside treated group compared with UV group. UV, ultraviolet; WT, wildtype; Asi, asiaticoside.

enhanced SOD activity, improving and restoring UV-induced changes in skin fibroblast appearance and cell structure. The present study found that asiaticoside downregulated ROS content and enhanced SOD activity, improving and restoring UV-induced changes in skin fibroblast appearance and cell structure. The inhibition of ROS content and the enhancement of SOD activity by asiaticoside were dose-dependent within a certain concentration range (40). Antioxidant enzymes such as SOD synergistically reduce ROS in organisms (41). Thus, the present study demonstrated that asiaticoside alleviated UV-induced photoaging in dermal cells by scavenging intracellular excess ROS.

Increased expression of MMPs is one of the major changes in skin photoaging (42). Under normal physiological conditions,

MMPs cooperate with tissue inhibitors of metalloproteinases to regulate ECM turnover to maintain cell stability (43). These proteins form the connective tissue of the skin's dermis. The role of MMPs in photoaging was initially discovered by observing that UV irradiation of human fibroblasts enhanced the expression of MMP-1, MMP-2, MMP-3, MMP-7, MMP-9 and MMP-36 (42,44). Therefore, MMPs are considered to be the key molecule of UV-induced aging (45). UVB radiation further induces elastic fibrosis and shrinks the extracellular matrix by inducing elastase and the expression of MMP-1, MMP-3 and MMP-9 (46,47). The present study demonstrated that the expression level of MMP-9 was significantly reduced in asiaticoside-treated HaCat cells compared with HaCat cells exposed to the same UV radiation.

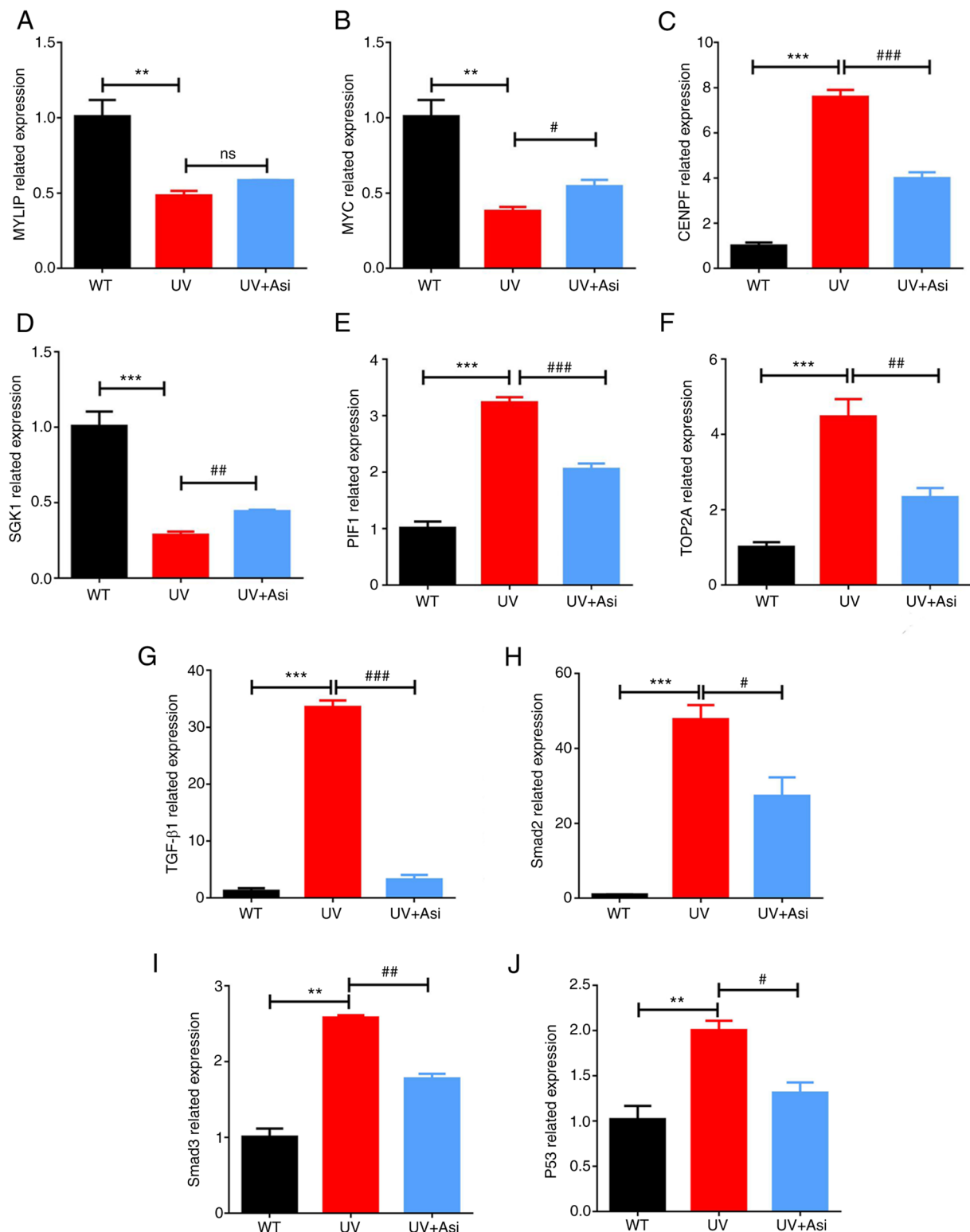


Figure 7. Transcriptional levels of (A) MYLIP; (B) MYC; (C) CENPF; (D) SGK1; (E) PIF, (F) TOP2A, (G) TGF- β 1, (H) Smad2, (I) Smad3 and (J) P53 mRNA were calculated by RT-qPCR. *significance of comparison between UV with WT group; #significance of comparison between treatment of asiaticoside in various doses with UV group. ** $P < 0.01$ and *** $P < 0.001$; # $P < 0.05$, ## $P < 0.01$ and ### $P < 0.001$. MYLIP, myosin regulatory light chain interacting protein; MYC, MYC proto-oncogene; CENPF, centromere protein F; SGK1, serum/glucocorticoid regulated kinase 1; PIF, phytochrome interacting factor; TOP2A, DNA topoisomerase II alpha.

UV-irradiated fibroblasts exhibit senescence characteristics (48). During cellular senescence, a major feature is the increased activity of lysosomal β -galactosidase, also known as Senescence-Associated β -galactosidase (SA- β -gal) (49).

β -galactosidase is the most frequently used signature molecule to identify aging in various *in vivo* and *in vitro* assays (50). The present study showed that UV radiation significantly increased the positive β -galactosidase in fibroblasts compared with

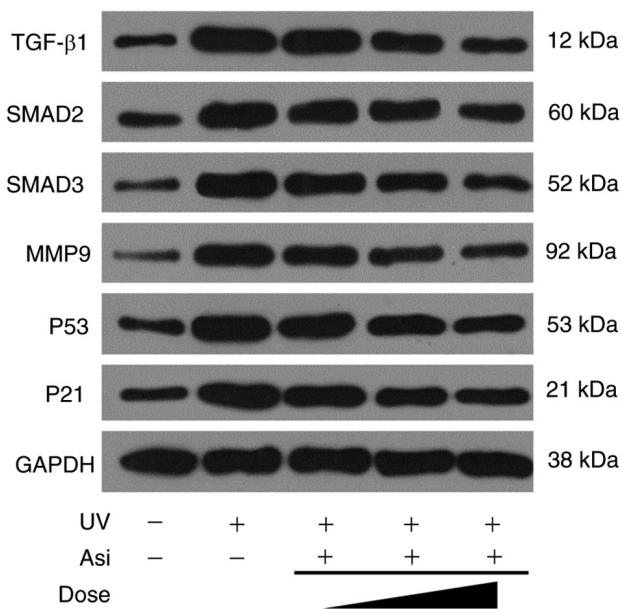


Figure 8. Western blot analysis of expression level of key proteins in TGF-β1/Smad and p53 pathways after treatment with UV and asiaticoside in various concentrations in HaCat cells. UV, ultraviolet; Asi, asiaticoside.

control cells, while the activity level of β-galactosidase was significantly reduced in a dose-dependent manner following asiaticoside treatment.

The present study then searched for the molecular mechanism of asiaticoside in relieving photoaging by RNAseq and finally focused on the TGF-β1/Smad signaling pathway, which is involved in a variety of cellular processes in organism and embryo development, including cell growth, cell differentiation, apoptosis and cellular homeostasis. Despite the wide range of cellular processes regulated by the TGF-β signaling pathway, the process is relatively simple (51,52). Smad protein is a family of 9 species currently known, Smad1-9, all of which have been found to be involved in the signal transduction of TGF-β. It is the downstream signal transduction molecule of its receptor, including receptor type, common mediator type, inhibitory type 3 categories. Smad complexes need to associate with other transcription factors to achieve transcriptional activation or repression of effector genes (53). A central part of TGF-β1 signaling is the SMAD-dependent canonical pathway: TGF-β triggers signaling through TGF-β type I receptors (TGF-βRI or ALK5) and TGF-β type II receptors (TGF-βRII), forming heterozygous tetramers, which subsequently activate downstream SMAD signaling proteins (54,55). The receptor-regulated SMAD/common-partner SMAD (R-SMAD/co-SMAD) complex accumulates in the nucleus, acts as a transcription factor and participates in the regulation of target gene expression.

The TGF/Smad pathway has an essential role in both natural aging and photoaging human skin and collagen is a key regulator of skin aging and wrinkle formation (56). The present study assessed the effect of asiaticoside on TGF-β1/Smad signaling pathway by western blotting. It was found that asiaticoside significantly reduced UV-mediated upregulation of TGF-β1, Smad2 and Smad3 compared with the control group.

With the improvement of understanding of asiaticoside, multiple functions of asiaticoside have been revealed. Not only capacity of anti-aging in UV damaged cells as reported in the present study, but also capability against retinal degradation and ameliorate inflammation through Nrf2/HO-1 pathway and TLR4/NF-κB pathway, respectively (57,58). Furthermore, asiaticoside-contained foam dressing, nano-composite and nanofibrous scaffold have been developed for traumatic treatment, showing great potential of asiaticoside in wound healing (14,59,60). By taking advantage of nanocarriers, novel usages of asiaticoside could be expanded and more applications related to asiaticoside might be developed. Thus, more basic research on asiaticoside is required for a comprehensive understanding of it.

Asiaticoside has significant therapeutic effects on skin photoaging, ameliorating and restoring UV-induced intracellular excess ROS in human skin cells and inhibiting the upregulation of TGF-β1, Smad2 and Smad3 by affecting the TGF-β1/Smad signaling pathway. Therefore, asiaticoside may be an effective strategy for the treatment of skin photoaging.

Acknowledgements

Not applicable.

Funding

The present study was supported by grant no. WX18B15 from Wuhan Municipal Health Commission.

Availability of data and materials

Raw data of RNA sequencing used in this study is available for downloading and analysis from public database Sequence Read Archive (<https://www.ncbi.nlm.nih.gov/Traces/study/>) with accession ID PRJNA851723. The data presented in this study are available on request from the corresponding author(s).

Authors' contributions

HJ, XZ and LC contributed to the design and research methods of this study. HJ performed experiments, analyzed results, drafted original manuscript and acquired research funding; XZ and LC reviewed and edited manuscript and administrated the whole project. XZ and LC confirm the authenticity of all the raw data. All authors have read and approved the final manuscript.

Ethics approval and consent to participate

Not applicable.

Patient consent for publication

Not applicable.

Competing interests

The authors declare that they have no competing interests.

References

- Rabe JH, Mamelak AJ, McElgunn PJ, Morison WL and Sauder DN: Photoaging: Mechanisms and repair. *J Am Acad Dermatol* 55: 1-19, 2006.
- Tobin DJ: Introduction to skin aging. *J Tissue Viability* 26: 37-46, 2017.
- Watson RE, Gibbs NK, Griffiths CE and Sherratt MJ: Damage to skin extracellular matrix induced by UV exposure. *Antioxid Redox Signal* 21: 1063-1077, 2014.
- Russo PA and Halliday GM: Inhibition of nitric oxide and reactive oxygen species production improves the ability of a sunscreen to protect from sunburn, immunosuppression and photocarcinogenesis. *Br J Dermatol* 155: 408-415, 2006.
- Hasham R, Choi HK, Sarmidi MR and Park CS: Protective effects of a *Ficus deltoidea* (Mas cotek) extract against UVB-induced photoaging in skin cells. *Biotechnology and Bioprocess Engineering* 18: 185-193, 2013.
- Sun L, Xu C, Lin P, Quigg A, Chin WC and Santschi PH: Photo-oxidation of proteins facilitates the preservation of high molecular weight dissolved organic nitrogen in the ocean. *Marine Chemistry* 229: 103907, 2021.
- Liu S, Mizu H and Yamauchi H: Proinflammatory responses to UV-irradiated ketoprofen mediated by the induction of ROS generation, enhancement of cyclooxygenase-2 expression and regulation of multiple signaling pathways. *Free Radic Biol Med* 48: 772-780, 2010.
- Wondrak GT, Roberts MJ, Cervantes-Laurean D, Jacobson MK and Jacobson EL: Proteins of the extracellular matrix are sensitizers of photo-oxidative stress in human skin cells. *J Invest Dermatol* 121: 578-586, 2003.
- Severino J, Allen RG, Balin S, Balin A and Cristofalo VJ: Is beta-galactosidase staining a marker of senescence in vitro and in vivo? *Exp Cell Res* 257: 162-171, 2000.
- Lee BY, Han JA, Im JS, Morrone A, Johung K, Goodwin EC, Kleijer WJ, DiMaio D and Hwang ES: Senescence-associated beta-galactosidase is lysosomal beta-galactosidase. *Aging Cell* 5: 187-195, 2006.
- Gary RK and Kindell SM: Quantitative assay of senescence-associated beta-galactosidase activity in mammalian cell extracts. *Anal Biochem* 343: 329-334, 2005.
- Gohil KJ, Patel JA and Gajjar AK: Pharmacological review on centella asiatica: A potential herbal cure-all. *Indian J Pharm Sci* 72: 546-556, 2010.
- George M, Joseph L and Ramaswamy: Anti-allergic, anti-pruritic and anti-inflammatory activities of *Centella asiatica* extracts. *Afr J Tradit Complement Altern Med* 6: 554-559, 2009.
- Namviriyachote N, Muangman P, Chinaroonchai K, Chuntrasakul C and Ritthidej GC: Polyurethane-biomacromolecule combined foam dressing containing asiaticoside: Fabrication, characterization and clinical efficacy for traumatic dermal wound treatment. *Int J Biol Macromol* 143: 510-520, 2020.
- Brinkhaus B, Lindner M, Schuppan D and Hahn EG: Chemical, pharmacological and clinical profile of the East Asian medical plant *Centella asiatica*. *Phytomedicine* 7: 427-448, 2000.
- Gao X, Lin J, Sun L and Ren Y: Clinical effects of dermatix ultra silica gel and asiaticoside cream on hyperplastic scar tissue in patients after epicanthoplasty. *Chinese J Medical Aesthetics and Cosmetology* 6: 508-511, 2019.
- Shukla A, Rasik AM, Jain GK, Shankar R, Kulshrestha DK and Dhawan BN: In vitro and in vivo wound healing activity of asiaticoside isolated from *Centella asiatica*. *J Ethnopharmacol* 65: 1-11, 1999.
- Kimura Y, Sumiyoshi M, Samukawa KI, Satake N and Sakanaka M: Facilitating action of asiaticoside at low doses on burn wound repair and its mechanism. *Eur J Pharmacol* 584: 415-423, 2008.
- Wijeweera P, Arnason JT, Koszycki D and Merali Z: Evaluation of anxiolytic properties of Gotukola- (*Centella asiatica*) extracts and asiaticoside in rat behavioral models. *Phytomedicine* 13: 668-676, 2006.
- Shubhra QTH, Oyane A, Araki H, Nakamura M and Tsurushima H: Calcium phosphate nanoparticles prepared from infusion fluids for stem cell transfection: Process optimization and cytotoxicity analysis. *Biomater Sci* 5: 972-981, 2017.
- Shubhra QTH, Kardos AF, Feczko T, Mackova H, Horák D, Tóth J, Dósa G and Gyenis J: Co-encapsulation of human serum albumin and superparamagnetic iron oxide in PLGA nanoparticles: Part I. Effect of process variables on the mean size. *J Microencapsul* 31: 147-155, 2014.
- Liu Y, Ding M, Guo K, Wang Z, Zhang C and Shubhra QTH: Systemic Co-delivery of drugs by a pH- and photosensitive smart nanocarrier to treat cancer by chemo-photothermal-starvation combination therapy. *Smart Materials in Medicine* 3: 390-403, 2022.
- Shubhra QTH, Guo K, Liu Y, Razzak M, Manir MS and Alam AKM: Dual targeting smart drug delivery system for multimodal synergistic combination cancer therapy with reduced cardiotoxicity. *Acta Biomater* 131: 493-507, 2021.
- Livak KJ and Schmittgen TD: Analysis of relative gene expression data using real-time quantitative PCR and the 2(-Delta Delta C(T)) method. *Methods* 25: 402-408, 2001.
- Guo K, Liu Y, Tang L and Shubhra QTH: Homotypic biomimetic coating synergizes chemo-photothermal combination therapy to treat breast cancer overcoming drug resistance. *Chemical Engineering J* 428: 131120, 2022.
- Su J, Guo K, Huang M, Liu Y, Zhang J, Sun L, Li D, Pang KL, Wang G, Chen L, *et al*: Fucoxanthin, a marine xanthophyll isolated from *conticribra weissflogii* ND-8: Preventive anti-inflammatory effect in a mouse model of sepsis. *Front Pharmacol* 10: 906, 2019.
- Guo K, Xiao N, Liu Y, Wang Z, Tóth J, Gyenis J, Thakur VK, Oyane A and Shubhra QTH: Engineering polymer nanoparticles using cell membrane coating technology and their application in cancer treatments: Opportunities and challenges. *Nano Materials Science*. 2021.
- Ji L, Xu J, Liu J, Amjad A, Zhang K, Liu Q, Zhou L, Xiao J and Li X: Mutant p53 promotes tumor cell malignancy by both positive and negative regulation of the transforming growth factor beta (TGF-beta) pathway. *J Biol Chem* 290: 11729-11740, 2015.
- Higgins SP, Tang Y, Higgins CE, Mian B, Zhang W, Czekay RP, Samarakoon R, Conti DJ and Higgins PJ: TGF- β /p53 signaling in renal fibrogenesis. *Cell Signal* 43: 1-10, 2018.
- Kuilman T, Michaloglou C, Mooi WJ and Peeper DS: The essence of senescence. *Genes Dev* 24: 2463-2479, 2010.
- Cavinato M and Jansen-Durr P: Molecular mechanisms of UVB-induced senescence of dermal fibroblasts and its relevance for photoaging of the human skin. *Exp Gerontol* 94: 78-82, 2017.
- Wang SQ, Setlow R, Berwick M, Polsky D, Marghoob AA, Kopf AW and Bart RS: Ultraviolet A and melanoma: A review. *J Am Acad Dermatol* 44: 837-846, 2001.
- Debaq-Chainiaux F, Borlon C, Pascal T, Royer V, Eliaers F, Ninane N, Carrard G, Friguet B, de Longueville F, Boffe S, *et al*: Repeated exposure of human skin fibroblasts to UVB at subcytotoxic level triggers premature senescence through the TGF-beta1 signaling pathway. *J Cell Sci* 118: 743-758, 2005.
- Chainiaux F, Magalhaes JP, Eliaers F, Remacle J and Toussaint O: UVB-induced premature senescence of human diploid skin fibroblasts. *Int J Biochem Cell Biol* 34: 1331-1339, 2002.
- Georgetti SR, Casagrande R, Vicentini FT, Baracat MM, Verri WA Jr and Fonseca MJ: Protective effect of fermented soybean dried extracts against TPA-induced oxidative stress in hairless mice skin. *Biomed Res Int* 2013: 340626, 2013.
- Ribeiro FM, Ratti BA, Dos Santos Rando F, Fernandez MA, Ueda-Nakamura T, de Oliveira Silva Lautenschlager S and Nakamura CV: Metformin effect on driving cell survival pathway through inhibition of UVB-induced ROS formation in human keratinocytes. *Mech Ageing Dev* 192: 111387, 2020.
- Graindorge D, Martineau S, Machon C, Arnoux P, Guittou J, Francesconi S, Frochet C, Sage E and Girard PM: Singlet oxygen-mediated oxidation during UVA radiation alters the dynamic of genomic DNA replication. *PLoS One* 10: e0140645, 2015.
- Zhao J, Shi J, Shan Y, Yu M, Zhu X, Zhu Y, Liu L and Sheng M: Asiaticoside inhibits TGF- β 1-induced mesothelial-mesenchymal transition and oxidative stress via the Nrf2/HO-1 signaling pathway in the human peritoneal mesothelial cell line HMrSV5. *Cell Mol Biol Lett* 25: 33, 2020.
- Luo P, Huang Q, Chen S, Wang Y and Dou H: Asiaticoside ameliorates osteoarthritis progression through activation of Nrf2/HO-1 and inhibition of the NF- κ B pathway. *Int Immunopharmacol* 108: 108864, 2022.
- Proksch E, Schunck M, Zague V, Segger D, Degwert J and Oesser S: Oral intake of specific bioactive collagen peptides reduces skin wrinkles and increases dermal matrix synthesis. *Skin Pharmacol Physiol* 27: 113-119, 2014.
- Chen CC, Chiang AN, Liu HN and Chang YT: EGb-761 prevents ultraviolet B-induced photoaging via inactivation of mitogen-activated protein kinases and proinflammatory cytokine expression. *J Dermatol Sci* 75: 55-62, 2014.
- Pittayapruek P, Meehansan J, Prapapan O, Komine M and Ohtsuki M: Role of matrix metalloproteinases in photoaging and photocarcinogenesis. *Int J Mol Sci* 17: 868, 2016.

43. Nagase H, Visse R and Murphy G: Structure and function of matrix metalloproteinases and TIMPs. *Cardiovasc Res* 69: 562-573, 2006.
44. Kim MS, Kim YK, Cho KH and Chung JH: Regulation of type I procollagen and MMP-1 expression after single or repeated exposure to infrared radiation in human skin. *Mech Ageing Dev* 127: 875-882, 2006.
45. Brennan M, Bhatti H, Nerusu KC, Bhagavathula N, Kang SW, Fisher GJ, Varani J and Voorhees JJ: Matrix metalloproteinase-1 is the major collagenolytic enzyme responsible for collagen damage in UV-irradiated human skin. *Photochem Photobiol* 78: 43-48, 2003.
46. Vedrenne N, Coulomb B, Danigo A, Bonte F and Desmouliere A: The complex dialogue between (myo)fibroblasts and the extracellular matrix during skin repair processes and ageing. *Pathol Biol (Paris)* 60: 20-27, 2012.
47. Quan T, Qin Z, Xia W, Shao Y, Voorhees JJ and Fisher GJ: Matrix-degrading metalloproteinases in photoaging. *J Invest Dermatol Symp Proc* 14: 20-24, 2009.
48. Qin H, Zhang G and Zhang L: GSK126 (EZH2 inhibitor) interferes with ultraviolet A radiation-induced photoaging of human skin fibroblast cells. *Exp Ther Med* 15: 3439-3448, 2018.
49. Dimri GP, Lee X, Basile G, Acosta M, Scott G, Roskelley C, Medrano EE, Linskens M, Rubelj I and Pereira-Smith O: A biomarker that identifies senescent human cells in culture and in aging skin in vivo. *Proc Natl Acad Sci USA* 92: 9363-9367, 1995.
50. Hernandez-Segura A, Nehme J and Demaria M: Hallmarks of cellular senescence. *Trends Cell Biol* 28: 436-453, 2018.
51. Xu YR and Fisher GJ: Ultraviolet (UV) light irradiation induced signal transduction in skin photoaging. *J Dermatol Sci* 1: S1-S8, 2005.
52. Feczko T, Fodor-Kardos A, Sivakumaran M and Haque Shubhra QT: In vitro IFN- α release from IFN- α -loaded poly(lactic-co-glycolic acid) and pegylated poly(lactic-co-glycolic acid) nanoparticles. *Nanomedicine (Lond)* 11: 2029-2034, 2016.
53. Derynck R and Zhang YE: Smad-dependent and Smad-independent pathways in TGF- β family signalling. *Nature* 425: 577-584, 2003.
54. Sun ZW, Hwang E, Lee HJ, Lee TY, Song HG, Park SY, Shin HS, Lee DG and Yi TH: Effects of *Galla chinensis* extracts on UVB-irradiated MMP-1 production in hairless mice. *J Nat Med* 69: 22-34, 2015.
55. Hwang E, Lee DG, Park SH, Oh MS and Kim SY: Coriander leaf extract exerts antioxidant activity and protects against UVB-induced photoaging of skin by regulation of procollagen type I and MMP-1 expression. *J Med Food* 17: 985-995, 2014.
56. Varga J, Rosenbloom J and Jimenez SA: Transforming growth factor beta (TGF β) causes a persistent increase in steady-state amounts of type I and type III collagen and fibronectin mRNAs in normal human dermal fibroblasts. *Biochem J* 247: 597-604, 1987.
57. Park DW, Lee YG, Jeong YJ, Jeon H and Kang SC: Preventive effects against retinal degeneration by centella asiatica extract (CA-HE50) and asiaticoside through apoptosis suppression by the Nrf2/HO-1 signaling pathway. *Antioxidants (Basel)* 10: 613, 2021.
58. Gao L, Yang M, Cai S, Gao L, Gui C and Zhang Q: Asiaticoside regulates toll-like receptor 4/nuclear factor-Kappa B signaling pathway to relieve lipopolysaccharide-Induced inflammation and apoptosis in ATDC5 cells. *Current Topics in Nutraceuical Research* 19: 432, 2021.
59. Raharjo AB, Putra RDA, Indayaningsih N, Srifiana Y, Hardiansyah A, Irmawati Y, Widodo H and Destyorini F: Preparation of polyvinyl alcohol/asiaticoside/chitosan membrane nano-composite using electrospinning technique for wound dressing. *AIP Conference Proceedings* 2256: 030023, 2020.
60. Anand S, Rajinikanth PS, Arya DK, Pandey P, Gupta RK, Sankhwar R and Chidambaram K: Multifunctional biomimetic nanofibrous scaffold loaded with asiaticoside for rapid diabetic wound healing. *Pharmaceutics* 14: 273, 2022.



This work is licensed under a Creative Commons Attribution-NonCommercial-NoDerivatives 4.0 International (CC BY-NC-ND 4.0) License.